J Inorg Organomet Polym (2012) 22:903–909
DOI 10.1007/s10904-012-9658-z

COMMUNICATION

Synthesis and Structural Characterization of New Lead(II) Discrete and Infinite Cage-Like Framework: A Precursor to Produce Pure Phase Nano-Sized Lead(II) Oxide

Gholam Hossein Shahverdizadeh · Fateme Hakimi · Babak Mirtamizdoust · Aliakbar Soudi · Pejman Hojati-Talemi

Received: 9 November 2011 / Accepted: 18 January 2012 / Published online: 1 February 2012

Abstract A novel Pb(II) complex, $\{[Pb_2(tpmba)_2(NO_3)_4]\cdot MeOH\}_n$ (**1**), was obtained by the reaction of a tripodal ligand, *N*,*N*′,*N*″-tris(pyrid-3-ylmethyl)-1,3,5-benzenetricarboxamide (tpmba), with $Pb(NO_3)_2$. The structure of complex was determined by X-ray crystallography. The results of structural analysis of the complex reveal that **1** is a M_2L_2 cage-like with a methanol molecule beside the cage. An entirely different structure and topology between **1** and similar complexes indicate that the nature of organic ligands affects the structure of assemblies. The results indicate that the framework of this complex is predominated by the nature of the organic ligand, anions, solvent and geometric need of the metal ions. It was found that the coordination number of Pb^{II} ions is eight, (PbN_3O_5) has a stereo-chemically active electron lone pair and the coordination sphere is hemi-directed. PbO nanoparticles are obtained by thermolysis of **1** at 180 °C with oleic acid as a surfactant. Scanning electron microscopy shows that the size of the PbO particles is ~30 nm.

G. H. Shahverdizadeh (✉)
Department of Chemistry, Faculty of Science, Tabriz Branch, Islamic Azad University, P.O. Box 1655, Tabriz, Iran
e-mail: Shahverdizadeh@iaut.ac.ir

F. Hakimi · B. Mirtamizdoust · A. Soudi
Department of Chemistry, University of Zanjan, Zanjan, Iran

B. Mirtamizdoust (✉)
Department of Inorganic Chemistry, Faculty of Chemistry, University of Tabriz, P.O. Box 5166616471, Tabriz, Iran
e-mail: tamizdoust@tabrizu.ac.ir

P. Hojati-Talemi
Mawson Institute, University of South Australia, Mawson Lakes SA 5095, Australia

Keywords Lead(II) · Cage compounds · Tripodal ligands · Nano lead(II) oxide

1 Introduction

In recent years, numerous studies of porous coordination polymers (PCPs), also called metal-organic frameworks (MOFs), have been reported because of their applications in gas adsorption, molecular storage and heterogeneous catalysis [1–4]. The appropriate design of ligands and metal building units have led to various interesting porous MOFs [5]. However, control of the shape and properties of the cavity formed is still challenging. Small changes in the building unit can lead to a completely different framework topology rather than an isostructural network with tuned cavity shape and properties. PCPs have characteristics that include (1) well-ordered porous structures, (2) flexible and dynamic behavior in response to guest molecules and (3) designable channel surface functionalities. Although channel surface modification is essential for the creation of functionalized porous structures, application of this synthetic approach to the PCP system has received little attention. Two types of strategies are used to functionalize channel surfaces: immobilization of coordinatively unsaturated (open) metal sites (OMS) and introduction of organic groups to provide guest-accessible functional organic sites (FOS) [6, 7]. There is a growing interest in the use of OMS for Lewis acid catalysis and specific gas adsorption, but less attention has been paid to the study of FOS despite their importance. The paucity of information on FOS is because of the difficulty of producing guest-accessible FOS on the pore surface: these organic groups tend to coordinate metal ions via a self-assembly process, resulting in frameworks in which FOS are completely blocked.

PCPs with amide groups are candidate compounds that have FOS as guest interaction sites. The amide group is a fascinating functional group because it possesses two types of hydrogen bonding sites: the –NH moiety acts as an electron acceptor [8, 9]. These multifunctional moieties of amide groups tend to form hydrogen bonds among themselves and interact negligibly with guest molecules after construction of PCPs. If a PCP could be prepared without forming amide–amide interactions, these groups would constitute attractive interaction sites for selective sorption and/or catalysis inside the channel. To retain amide groups as guest interaction FOS inside the network, we employed a three-connector ligand containing amide groups. Three-connector ligands are more useful for construction of 3D PCPs with coordination bonds than bidentate or monodentate ligands [10]. Additionally, lead(II) frameworks have attracted great interest because of lead's large ion radius, a variable coordination number, the possible occurrence of a stereo-chemically active lone pair of $6s^2$ outer electrons and novel network topologies [11, 12]. According to the hard-soft acid–base theory, the intermediate coordination ability of lead(II) means that it can flexibly coordinate small nitrogen or oxygen atoms as well as large sulfur atoms [13]. The investigation of stereochemical activity of the valence shell electron lone pairs in polymeric and supramolecular compounds may be more interesting as the spontaneous aggregation of several bridging ligands may cause the gap to disappear and leading to a less common holo-directed arrangement [14].

Lead(II) coordination polymers have been previously studied in some extent [15–18]. We have recently focused our attention on the design and synthesis of metal–organic frameworks with specific topologies and properties by using a flexible tripodal ligand containing three pyridyl groups as coordination sites and three amide groups as guest interaction sites; e.g., (*N*,*N*′,*N*″-tris(pyrid-3-ylmethyl)-1,3,5-benzenetricarboxamide (tpmba, Scheme 1) [19]. In order to study further the assembly of the flexible tripodal ligand with post-transition metal salts and the inclusion properties of MOFs, we synthesized and characterized the Pb(II) complex with this ligand. In this paper, we report the crystal structure and inclusion properties of $\{[Pb_2(tpmba)_2(NO_3)_4]\cdot MeOH\}_n$ (**1**) and their conversion into nano-structured lead oxide using calcination at moderately elevated temperatures. In recent years many kinds of lead(II) coordination polymers have been prepared by the several methods. It should be emphasized that there are different methods to synthesize nano- and micro-crystalline lead(II) oxide such as microwave-solvothermal synthesis, hydrothermal route and surfactant ligand co-assisting solvothermal synthesis [20–26].

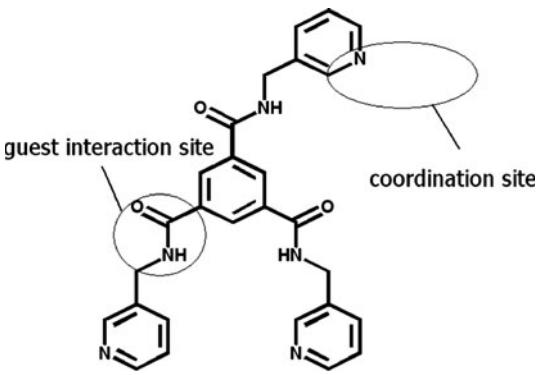

Scheme 1 *N*,*N*′,*N*″-tris(pyrid-3-ylmethyl)-1,3,5-benzenetricarboxamide (tpmba)

2 Experimental

2.1 Physical Property Measurements

The ligand tpmba was prepared as described previously [11, 27]. All other reagents and solvents were commercially available and were used without further purification. An Elementar Vario Microanalyzer CHN–O-Rapid Analyzer was used for C, H and N elemental analysis of samples. The IR spectra were performed on a Bruker Vector 22 FT-IR spectrometer disks in the 4,000–400 cm^{-1} range as KB disks. Thermogravimetric–differential scanning calorimetry (TGA/DSC) curves were recorded on SETARAM LABSYS Thermal analyser from 25–800 °C under a N_2 flow; heating rate, 3 °C min^{-1}. X-ray powder diffraction (XRD) measurements were performed using an X'pert diffractometer (Panalytical) with monochromatized CuK_α radiation. The crystallite sizes of selected samples were estimated using the Scherrer formula. The morphology of samples after gold coating was investigated using a scanning electron microscope (Philips XL 30). Crystallographic measurements were made at 100(2) K using a Bruker SMART CCD area detector diffractometer. The intensity data were collected using graphite monochromated MoK_α radiation ($\lambda = 0.71073$ Å). Accurate unit cell parameters and orientation matrix for data collection was obtained from least–squares refinement. The structure has been solved by direct methods and refined by full-matrix least-squares techniques on F^2.

2.2 Synthesis of $\{[Pb_2(tpmba)_2(NO_3)_4]\cdot MeOH\}_n$

A solution of tpmba (36.0 mg, 0.075 mmol) in methanol (15 mL) was added to an aqueous solution of $Pb(NO_3)_2$ (0.075 mmol mL^{-1}, 1 mL). The mixture was stirred for 0.5 h, then filtered. Colorless crystals were obtained after the filtrate was allowed to stand for several weeks; yield, 58%. Elemental analysis, calc. (%) for $C_{28}H_{28}N_8O_{10}Pb$: C: 39.86, H: 3.34, N: 13.28; found: C: 40.00, H: 3.40, N:

Scheme 2 Materials produced and synthetic methods

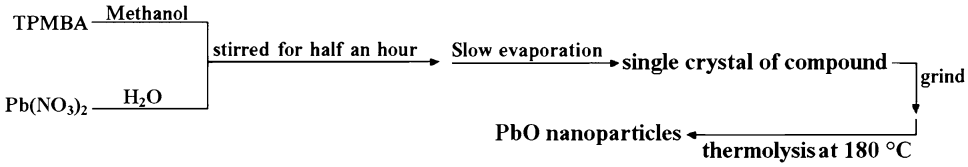

Table 1 Crystal data and structure refinement for $\{[Pb_2(tpmba)_2(NO_3)_4]\cdot MeOH\}_n$ (**1**)

Empirical formula	$C_{28}H_{28}N_8O_{10}Pb$
Formula weight	843.77
Temperature	100(2) K
Wavelength	0.71073 Å
Crystal system	Monoclinic
Space group	$P2_1/n$
Unit cell dimensions	$a = 18.3145(15)$ Å
	$b = 7.8110$ (7) Å
	$c = 20.7812$ (18) Å
	$\beta = 93.958$ (2)°
Volume	2965.8 (4) Å^3
Z	4
Density (calculated)	1.890 Mg/m^3
Absorption coefficient	5.762 mm^{-1}
$F(000)$	1656 e
Crystal size	0.41 × 0.19 × 0.12 mm^3
θ range for data collection	1.43°–31.26°
Index ranges	$-25 \le h \le 13, -11 \le k \le 11, -29 \le l \le 29$
Reflections collected	8,709
Independent reflections	7232 [R(int) = 0.0493]
Refinement method	Full-matrix least-squares on F^2
Goodness-of-fit on F^2	1.069
Final R indices	$R1 = 0.0475$, $wR2 = 0.0761$
$[I > 2\sigma(I)]$	
R indices (all data)	$R1 = 0.0355$, $wR2 = 0.0711$

Table 2 Selected bond lengths and bond angles for $\{[Pb_2(tpmba)_2(NO_3)_4]\cdot MeOH\}_n$

N8 Pb1	2.703 (3)	O3 Pb1	2.643 (3)
O4 Pb1	2.677 (3)	O2 Pb1	2.661 (3)
Pb1 N6	2.620 (4)	Pb1 N3	2.5169 (3)
Pb1 O1	2.902 (3)	Pb1 O3^i	2.916 (3)
C1 N3 Pb1	117.1 (3)	C5 N3 Pb1	124.4 (3)
C20 N6 Pb1	124.2 (3)	C19 N6 Pb1	117.8 (3)
C27 N8 Pb1	113.8 (3)	C26 N8 Pb1	128.2 (3)
N1 O3 Pb1	102.9 (2)	N2 O4 Pb1	96.3 (2)
N2 O6 Pb1	97.1 (2)	N3 Pb1 N6	80.40 (12)
N3 Pb1 O3	71.34 (11)	N6 Pb1 O3	73.55 (11)
N3 Pb1 O6	79.56 (10)	N6 Pb1 O6	72.44 (11)
O3 Pb1 O6	138.14 (9)	N3 Pb1 O4	79.35 (11)
N6 Pb1 O4	119.54 (11)	O3 Pb1 O4	145.48 (10)
O6 Pb1 O4	48.10 (9)	N3 Pb1 N8	86.48 (11)
N6 Pb1 N8	155.07 (11)	O3 Pb1 N8	82.21 (11)
O6 Pb1 N8	125.94 (10)	O4 Pb1 N8	78.12 (10)
O6 Pb1 O1	154.95 (3)		

13.30. FT-IR v, cm^{-1} (selected band): 3494 (br), 3188 (s), 2922 (w), 2160 (w), 2028 (w), 1978 (w), 1668 (s), 1615 (w), 1587 (m), 1544 (s), 1488 (s), 1423 (s), 1350 (s), 1242 (m), 1088 (s), 1011 (s), 951 (m), 933 (m), 811 (m), 734 (w), 697 (m), 651 (w), 622 (w) cm^{-1}.

2.3 Synthesis of PbO Nanoparticles

Compound **1** (0.1 mmol) was ground and dissolved in oleic acid (1.58 mL) to form a pale yellow solution. This solution was degassed for 20 min and heated to 180 °C for 2 h. A black precipitate formed. A small amount of toluene and a large excess of EtOH were added to the reaction solution and PbO nanoparticles were separated by centrifugation. The solids were washed with EtOH and dried in air.

3 Results and Discussion

Reaction between TPMBA) and lead(II) nitrate in methanol solution provides crystalline material that is analyzed as $\{[Pb_2(tpmba)_2(NO_3)_4]\cdot MeOH\}_n$. Scheme 2 gives an overview of the methods used for the synthesis of $\{[Pb_2(tpmba)_2(NO_3)_4]\cdot MeOH\}_n$ (**1**) and PbO nanoparticles. The IR spectrum of these compounds show characteristic bands of tpmba and methanol. For example, a band at 1,350 cm^{-1} is due to the presence of the NO_3^- stretching vibration; a broad band at 3,494 cm^{-1} is assigned to the O–H stretching vibration in methanol, and a strong band at 3,188 cm^{-1} is assigned to the N–H. stretching vibration. The strong band at 1,668 cm^{-1} is due to the C=O group stretching vibration of the tpmba ligand [28].

The structure of the complex is determined by X-ray crystallography. The crystallographic data are summarized in Table 1. Selected bond lengths and bond angles are shown in Table 2. Thus, the X-ray crystallographic analysis shows that complex **1** crystallized in the monoclinic system with space group of $P2_1/n$ and has a cage-like structure [29]. The molecular structure of an asymmetric unit and two views of the $[Pb_2(tpmba)_2(NO_3)_4]$.MeOH unit are shown in Fig. 1. The coordination number of each Pb(II)-atoms in **1** is eight; each Pb(II) is coordinated to

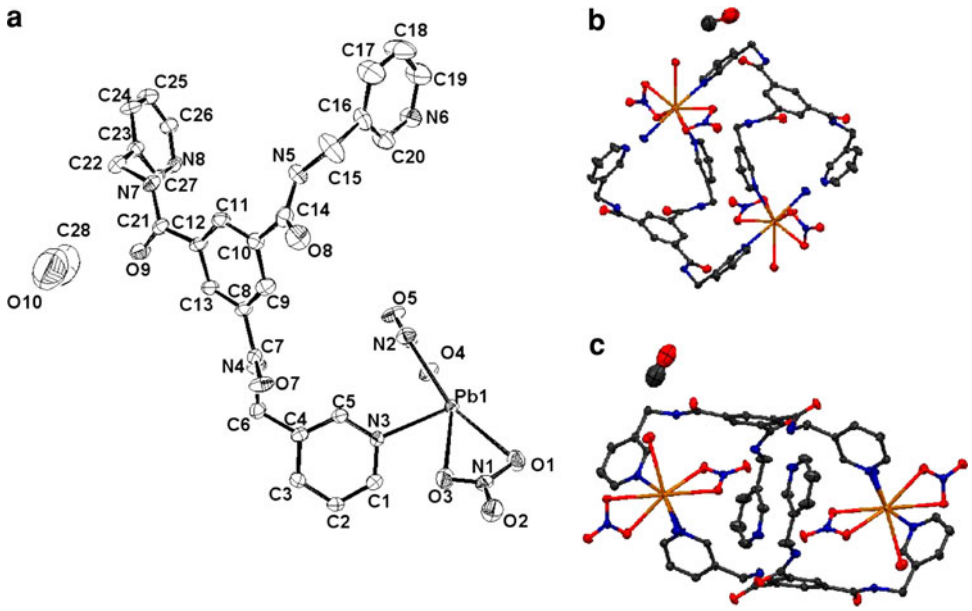

Fig. 1 **a** Molecular structure of the asymmetric unit; **b**, **c**: two view of the $[Pb_2(tpmba)_2(NO_3)_4]\cdot MeOH$ unit

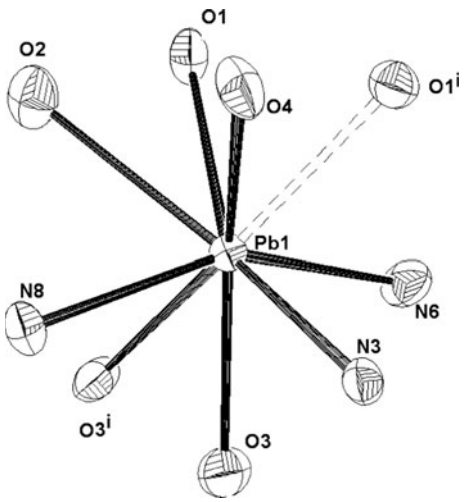

Fig. 2 Schematic representation of the Pb^{II} environment

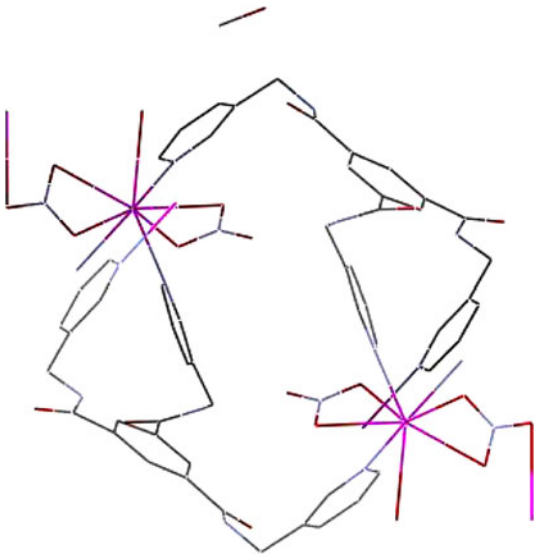

Fig. 3 Distorted 4-membered ring composed of three octahedral Pb(II) linked together by tow tpmba units

three pyridyl N-atoms with Pb–N distances of 2.5169(3), 2.703(3) and 2.620(4) Å and five nitrate O-atoms with Pb–O distance of 2.677(3), 2.661(3), 2.643(3), 2.902(3) and 2.916(3) Å. The arrangement of these ligands suggests the presence of a gap or a hole in the coordination geometry around the metal ions (O6–Pb1–O1 = 154.95(3)), possibly occupied by a *stereo-active* lone pair of electrons on Pb(II) [29]. The observed shortening of the Pb–N bonds on the side of Pb(II) ion opposite to the putative lone pair of electrons (N3–Pb1 = 2.5169(3) Å compared to $O3^i$–Pb1 = 2.916(3) Å adjacent to the lone pair) supports the presence of the gap [29–33]. Thus, the geometry of the nearest coordination environment of each lead atom is most likely caused by the geometrical constraint of the coordinated tpmba ligand, nitrate anions and the influence of a stereo-chemically active lone pair of electrons in hybrid orbital on the metal atom. Such an environment leaves space for bonding of another oxygen atom of the nitrate anion. To find any potential donor center within this vacancy, the bonding limit needs to be extended at least 3.1 Å [30]. Hence, It is possible to locate nitrate O-atoms approaching each Pb (i.e., $Pb1\cdots O1^i$ = 2.939 Å) (Fig. 2). Therefore, the coordination sphere is almost complete; and, the coordination number will be nine (PbN_3O_6) with holo-directed geometry [30] (symmetry code: $i = -x, -y, -z$).

The framework of complex **1** was constructed from the Pb(II) center as an eight-connected node. This arrangement produces a large four-membered ring composed of two octahedral Pb(II) moieties linked together by two tpmba

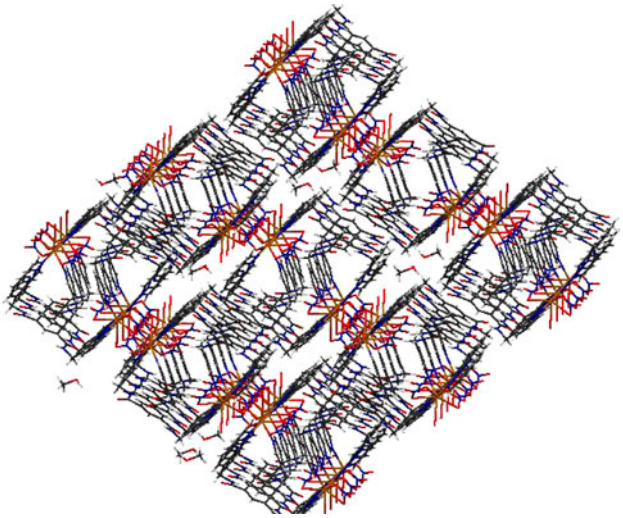

Fig. 4 Framework expanded in three directions to form a 3D framework

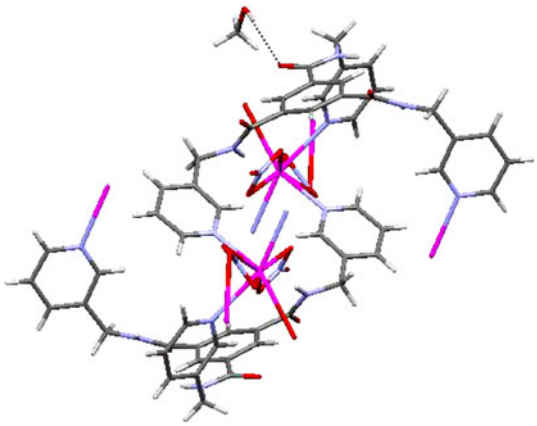

Fig. 6 Representation of the hydrogen bonds of methanol with the NH group of the amide groups

units (M_2L_2). The rotation of tpmba between the benzene ring and amide group (Fig. 3) results in rotation of the four-membered ring. The framework expands in three directions with a Pb(II)···Pb(II) separation of 11.095 Å to form a 3D network (Fig. 4). Two frameworks mutually interpenetrating with the nearest-neighbor Pb(II)···Pb(II) distance of 5.710 Å between Pb(II)-atoms in the adjacent frameworks produces three-dimensionally running channels (3D pores) with dimensions of 9.915 × 12.723 $Å^2$. These pores are available and suitable for guest molecule accommodation and exchange (Fig. 5). The channel is not straight. The nearest N(amide)-to-N(amide) distances are about 13.557 Å in the network and 5.220 Å between the two adjacent networks while the distance of N(amide)-to-O(amide) is about 6.408 Å. Consequently, the highly ordered amide groups on the surfaces of the channels could act as important FOS in the interaction between the host and guest molecules. The X-ray crystallographic results clearly show that methanol molecules interact with the NH moieties of the amide groups (O[methanol]···N[amide]) ca. 2.829 Å) via hydrogen bonds (Fig. 6).

To study the thermal stability of **1**, the thermogravimetric analysis (TGA) under nitrogen from 25 to 580 °C was performed on polycrystalline samples. The TG curve shows that **1** is thermally stable to 261 °C and then loses the organic ligand and solvent to 411 °C. A solid residue of PbO occurs when **1** is heated at 600 °C.

PbO powders weren generated by thermal decomposition of **1** in air. The powder XRD patterns (Fig. 7) match with the standard pattern of orthorhombic PbO with $a = 5.8931$ Å and $z = 4$ (JCPDS card file No. 77-1971) and confirms the formation of PbO. Significant broadening of the peaks indicate that the particles are of nanometer dimensions. The average size of the particles is 30 nm and is estimated from the Scherrer formula ($D = 0.891\lambda/\beta\cos\theta$, where D is the average grain size, λ is the X-ray wavelength (1.5418 Å), θ is the diffraction angle and β is the full-width at half maximum of an observed peak). The morphology and size of the PbO samples were further investigated with SEM. A bulk powder sample of **1** produces regularly shaped Pb(II) oxide nanoparticles with a diameter about 30 nm (Fig. 8), which is comparable to similarly reported preparations [20–26].

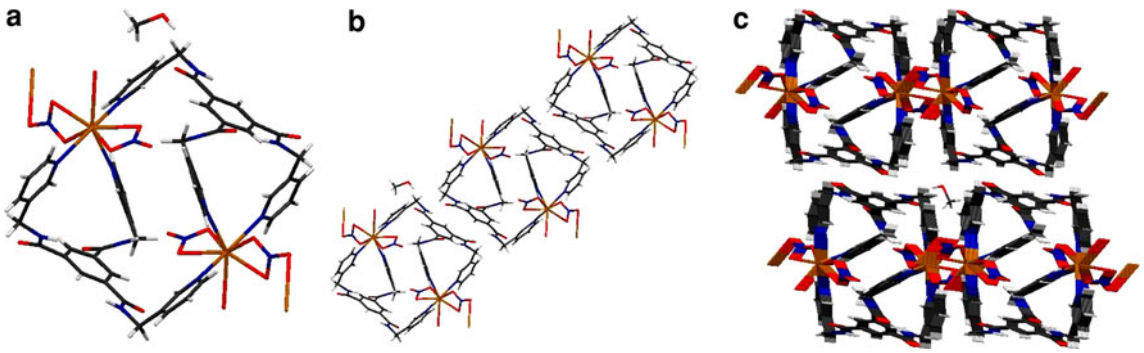

Fig. 5 **a–c** Two-fold interpenetrating 3D crystal structure

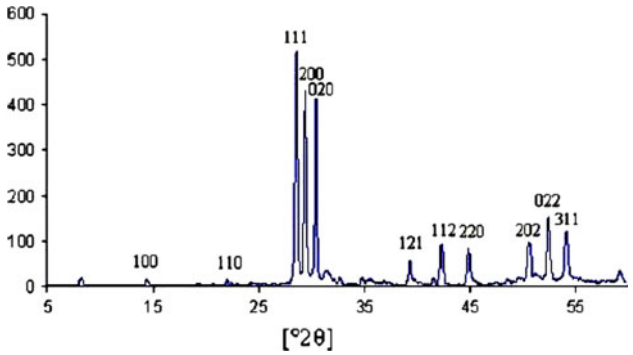

Fig. 7 XRD patterns of PbO after calcination of **1**

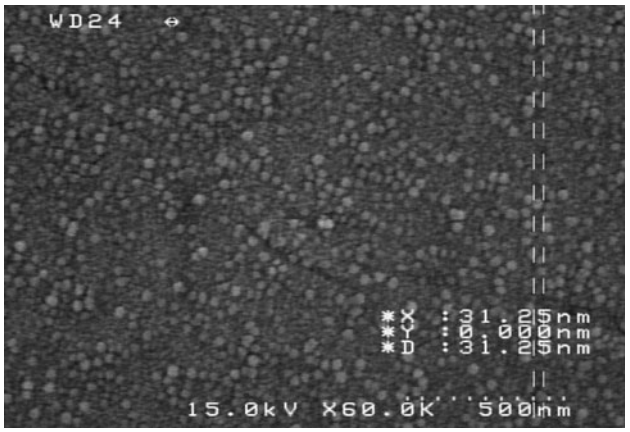

Fig. 8 SEM photographs of PbO nano-powders (produced by calcination of compound $\{[Pb_2(tpmba)_2(NO_3)_4]\cdot MeOH\}_n$ (**1**)

4 Conclusion

This study describes the construction of a 3D PCP-containing guest-accessible amide groups. A 3D PCP that is functionalized with amide groups, $\{[Pb_2(tpmba)_2(NO_3)_4]\cdot MeOH\}_n$ (**1**), was successfully synthesized from the reaction of $Pb(NO_3)_2$ and a three connector-type amide ligand (tpmba). The structure of the product was characterized by X-ray crystallographic analysis. The result of structural analysis of complex revealed that **1** was a M_2L_2 type cage-like complex with a methanol molecule beside the cage. The framework of **1** was constructed from the Pb(II) center as an eight-connected node. This arrangement produces a large four-membered ring composed of tow octahedral Pb(II) moieties linked together by tow tpmba units. The four-membered ring is distorted because of the rotation of tpmba between the benzene ring and the amide group. The framework expands in three directions, with a Pb(II)···Pb(II) separation of 11.095 Å. The channel is not straight.

The arrangement of these ligands suggests presence gap or a hole in coordination geometry around the Pb(II) ions. It is possible to find nitrate-oxygen atoms approaching each Pb ($Pb1\cdots O1^{i} = 2.939$ Å); therefore, the coordination sphere is almost completed and the coordination number will be nine (PbN_3O_6) with holo-directed geometry. In this case the PbO nanoparticles were obtained by thermolysis of **1** at 180 °C with oleic acid as a surfactant. The scanning electron microscopy shows that the size of the PbO particles is ~30 nm.

5 Supplementary Material

Crystallographic data for the structure reported in the paper has been deposited with the Cambridge Crystallographic Data Centre as supplementary publication No. CCDC-807076 for $\{[Pb_2(tpmba)_2(NO_3)_4]\cdot MeOH\}_n$. Copies of the data can be obtained on application to CCDC, 12 Union Road, Cambridge CB2 1EZ, UK [Fax: +44–1223/336033; e-mail: deposit@ccdc.cam.ac.uk].

Acknowledgments The authors thank Islamic Azad University, University of Zanjan and the University of Tabriz for their support. We also thank Dr Abrahams for his assistance in the X-ray crystallography.

References

1. M.J. Rosseinsky, Microporous Mesoporous Mater. **73**, 15 (2004)
2. M. Dinca, J.R. Long, J. Am. Chem. Soc. **127**, 9376 (2005)
3. H. Kim, M.P. Suh, Inorg. Chem. **44**, 810 (2005)
4. T. Uemura, R. Kitaura, Y. Ohta, M. Nagaoka, S. Kitagawa, Angew. Chem. Int. Ed. **45**, 4112 (2006)
5. N.W. Ockwig, O. Delgado-Friedrichs, M. O'Keeffe, O.M. YaghiAcc, Chem. Res. **38**, 176 (2005)
6. S.H. Cho, B. Ma, S.T. Nguyen, J.T. Hupp, T.E. Albrecht-Schmitt, Chem. Commun. 2563 (2006)
7. R. Custelcean, M.G. Gorbunova, J. Am. Chem. Soc. **127**, 16362 (2005)
8. B.C. Tzeng, B.S. Chen, H.T. Yeh, G.H. Lee, S.M. Peng, New J. Chem. **30**, 1087 (2006)
9. P.L. Huyskens, J. Am. Chem. Soc. **99**, 2578 (1977)
10. O. Ohmori, M. Kawano, M. Fujita, J. Am. Chem. Soc. **126**, 16292 (2004)
11. L. Shimoni-Livny, J.P. Glusker, C.W. Brock, Inorg. Chem. **37**, 1853 (1998)
12. L.M. Engelhardt, B.M. Furphy, J.M. Harrowfield, J.M. Patrick, A.H. White, Inorg. Chem. **28**, 1410 (1989)
13. C. Platas-Iglesias, D. Esteban-Gomez, T. Enriquez-Perez, F. Avecilla, A. deBlas, T. Rodriguez-Blas. Inorg. Chem. **44**, 2224 (2005)
14. S. Taheri, A. Mojidov, A. Morsali, Z. Anorg, Allg. Chem. **633**, 1949 (2007)
15. Z. Chen, J. Yan, H. Xing, Z. Zhang, F. Liang, J. Solid State Chem. **184**, 1063 (2011)
16. H. Sadeghzadeh, A. Morsali, V.T. Yilmaz, O. Büyükgüngr, Mater Lett **64**, 810 (2010)
17. D. Li, X. Liu, J. Zhou, Inorg. Chem. Commun. **11**, 367 (2008)
18. A.M. Puthan Peedikakkal, J.J. Vittal, Inorg. Chem. **49**, 10 (2010)
19. J. Fan, H. Zhu, T. Okamura, W. Sun, W. Tang, N. Ueyama, Chem. Eur. J. **9**, 4724 (2003) and references therein.
20. K. Akhbari, A. Morsali, Cryst. Eng. Comm. **13**, 2047 (2011)

21. L. Hashemi, A. Morsali, P. Retailleau, Inorg. Chim. Acta **367**, 207 (2011)
22. H. Sadeghzadeh, A. Morsali, Ultrason. Sonochem. **18**, 80 (2011)
23. L. Aboutorabi, A. Morsali, Ultrason. Sonochem. **18**, 407 (2011)
24. M. J. Soltanian fard, A. Morsali, J. Inorg. Organomet. Polym. **20**, 727 (2010).
25. L. Hashemi, A. Morsali, J. Inorg. Organomet. Polym. **20**, 856 (2010)
26. H. Sadeghzadeh, A. Morsali, J. Inorg. Organomet. Polym. **20**, 733 (2010)
27. R. Kannappan, D.M. Tooke, A.L. Spek, J. Reedijk, J. Mol. Struct. **751**, 55 (2005)
28. K. Nakamoto, *Infrared and Raman Spectra of Inorganic and Coordination Compounds'*, 5th edn. (Wiley, New York, 1997)
29. L. Shimoni-Livny, J.P. Glusker, C.W. Brock, Inorg. Chem. **37**, 1853 (1998)
30. R.D. Hancock, M.S. Shaikjee, S.M. Dobson, J.C.A. Boeyens, Inorg. Chim. Acta **154**, 229 (1998)
31. F. Marandi, B. Mirtamizdoust, A.A. Soudi, V.T. Yilmaz, C. Kazak, Z. Anorg, Allg. Chem. **632**, 2380 (2006)
32. B. Shaabani, B. Mirtamizdoust, M. Shadman, H. –K. Fun. Z. Anorg. Allg. Chem. **635**, 2642 (2009)
33. B. Shaabani, B. Mirtamizdoust, D. Viterbo, G. Croce, H. Hammud, P. Hojati-Lalemi, A. Khandar, Z. Anorg. Allg. Chem. **637**, 713 (2011)